Estimating the Baroreflex and Respiratory Modulation of Peripheral Vascular Resistance

Patjanaporn Chalacheva-*IEEE Student Member* and Michael C.K. Khoo, *IEEE Fellow*

***Abstract*— The peripheral vascular resistance (R_{PV}) control is known to be largely sympathetically-mediated; thus assessment of the R_{PV} control would allow us to infer valuable information regarding sympathetic nervous activity. The linear and 2nd-order nonlinear minimal models were used to capture the influences of blood pressure (baroreflex) and respiration (respiratory-coupling) on fluctuations of R_{PV}. To validate the minimal models, they were applied on the "data" generated by the simulation model developed in our previous study. This study demonstrated that the linear minimal model was able to recover the "true" (simulated) kernels. The nonlinear model was able to detect the increase in nonlinearity in the system. The system gains derived from the estimated kernels showed strong relationship with the simulation gains, suggesting that the system gains could be employed as potential biomarkers of autonomic function. These results also showed that the nonlinear model had sufficient sensitivity to detect the difference in autonomic reactivity between subjects with mild and severe metabolic syndrome and obstructive sleep apnea syndrome exposed to orthostatic stress.**

I. Introduction

Assessment of sympathetic nervous activity (SNA) has been an important focus of medical research, as knowledge of sympathetic activity provides information not only about the underlying autonomic physiology, but also about the clinical state of the subject being tested. Various techniques have been developed for the assessment of SNA but these techniques can be invasive, costly, and/or technically demanding. Since the peripheral vascular resistance (R_{PV}) is known to be sympathetically mediated [1] and the changes in R_{PV} are reflected as vasoconstriction/vasodilation response, SNA information can be inferred from these responses. Vasoconstriction response can be measured noninvasively by devices such as peripheral arterial tonometry (PAT) and Laser Doppler flowmeter. Thus, we could potentially employ the detection of vasoconstriction response as an indicator of changes in SNA.

The regulation of R_{PV} is generally attributed to the baroreflex control of total peripheral resistance (TPR). However, evidence shows strong respiratory modulation on muscle sympathetic nerve activity measured from peroneal nerve [2, 3]. Also, a deep breath or a sigh is reported to be rather consistently followed by peripheral vasoconstriction [4, 5], which further suggests a modulatory influence of respiration on R_{PV}. To confirm this observation, our previous study employed a minimal modeling approach to investigate whether the respiratory modulation on R_{PV} was a result of the modulatory effect of respiration on blood pressure, whose effect got carried over to be reflected in R_{PV}, or it was a result of direct modulation of respiration [6]. We found that respiration likely affects R_{PV} through direct modulation [6]. Further, the closed-loop simulation model of blood pressure variability developed in the previous study was able to demonstrate that without incorporating the respiratory modulation effect on TPR, the sigh-vasoconstriction response cannot be reproduced [6].

In this study, we validated the minimal model its ability to capture the variability in R_{PV}. This was achieved by applying the minimal model on "data" generated by the simulation developed in the previous study to see whether the simulated ("true") impulse responses could be recovered. We also extended the minimal model proposed in the previous study to incorporate the 2nd-order nonlinear components as well as the blood pressure-respiration interaction. Lastly, we applied the minimal models of R_{PV} variability on experimental data obtained from obese children with varying degrees of metabolic syndrome (MetS) and obstructive sleep apnea syndrome (OSAS).

II. Methods

B. Minimal Models

Two minimal models were employed in this study: linear and 2nd-order nonlinear models. Both minimal models were assumed to be time-invariant models. The linear model consisted of two main autonomic-mediated mechanisms. The first one was the baroreflex control of peripheral vascular conductance (BPC), which related fluctuations in mean arterial pressure (MAP) to fluctuations in peripheral vascular conductance ($G_{PV} = 1/R_{PV}$). The second mechanism was the respiratory-peripheral vascular conductance coupling (RPC), which related fluctuations in respiration (ILV) to fluctuations in G_{PV}. The linear model can be represented as

$$\Delta G_{PV}(t) = \sum_{i=0}^{M-1} h_{BPC}(i)\Delta MAP(t-i-T_{BPC}) + \sum_{i=0}^{M-1} h_{RPC}(i)\Delta ILV(t-i-T_{RPC}) + \varepsilon_{G_{PV}}(t) \quad (1)$$

where h_{BPC} and h_{RPC} represent the impulse responses of BPC and RPC, respectively; T_{BPC} and T_{RPC} represent the latencies of BPC and RPC; M represents the memory of the system;

This work was supported in part by U.S. National Institute of Health grants HL090451 and EB001978.

P. Chalacheva is with the Biomedical Engineering Department, University of Southern California, Los Angeles, CA 90089 USA (phone: 213-740-0827; fax: 213-821-3897; e-mail: chalache@usc.edu).

M. C. K. Khoo is with the Biomedical Engineering Department, University of Southern California, Los Angeles, CA 90089 USA (e-mail: khoo@bmsr.usc.edu).

and $\varepsilon_{G_{PV}}$ represents the extraneous influence that cannot be explained by the model.

The 2nd-order nonlinear model included the quadratic nonlinear component of the BPC and RPC mechanisms as well as the interaction effect of the two inputs in addition to the linear components. The mathematical representation of the model is as follows:

$$\begin{aligned}\Delta G_{PV}(t) &= \sum_{i=0}^{M-1} h_{BPC}(i)\cdot \Delta MAP(t-i-T_{BPC}) \\ &+ \sum_{i=0}^{M-1} h_{RPC}(i)\cdot \Delta ILV(t-i-T_{RPC}) \\ &+ \sum_{i=0}^{M-1}\sum_{j=0}^{M-1} h_{2BPC}(i,j)\cdot \Delta MAP(t-i-T_{BPC})\cdot \Delta MAP(t-j-T_{BPC}) \\ &+ \sum_{i=0}^{M-1}\sum_{j=0}^{M-1} h_{2RPC}(i,j)\cdot \Delta ILV(t-i-T_{RPC})\cdot \Delta ILV(t-j-T_{RPC}) \\ &+ \sum_{i=0}^{M-1}\sum_{j=0}^{M-1} h_{BPC,RPC}(i,j)\cdot \Delta MAP(t-i-T_{BPC})\cdot \Delta ILV(t-j-T_{RPC}) \\ &+ \varepsilon_{G_{PV}}(t)\end{aligned} \quad (2)$$

where h_{BPC} and h_{RPC} represent the linear BPC and RPC; h_{2BPC} and h_{2RPC} represent the 2nd-order effect of blood pressure and respiration in G_{PV}, respectively; and $h_{BPC,RPC}$ represents the interaction of blood pressure and respiration on G_{PV}.

The model components (kernels) were estimated using the basis function expansion technique [7]. In brief, each kernel could be represented as a weighted sum of basis functions. In this case, Meixner basis functions (MBF) were chosen. Using this technique, each linear kernel can be represented as

$$h_x(t) = \sum_{j=1}^{q_x} c_x(j) B_j^{(n_x)}(t). \quad (3)$$

Each 2nd-order nonlinear kernel can be represented as

$$h_{xx}(t_1,t_2) = \sum_{i=1}^{q_x}\sum_{j=1}^{q_x} c_{xx}(i,j) B_i^{(n_x)}(t_1) B_j^{(n_x)}(t_2). \quad (4)$$

Lastly, the interaction kernel can be represented as

$$h_{xu}(t_1,t_2) = \sum_{i=1}^{q_x}\sum_{j=1}^{q_u} c_{xu}(i,j) B_i^{(n_x)}(t_1) B_j^{(n_u)}(t_2). \quad (5)$$

$B_i^{(n)}(t)$ and $B_j^{(n)}(t)$ are the orthonormal sets of MBF with n^{th} order of generalization. The larger the value of n, the longer it takes for the MBF to reach its maximum value. c_x correspond to the expansion coefficients of the basis functions for the linear kernel. c_{xx} and c_{xu} correspond to the expansion coefficients of the basis functions for the nonlinear kernel and interaction, respectively. q_x and q_u represent the Meixner function orders, the total numbers of MBF, used in the expansion of the kernels. The weights or the expansion coefficients of the basis functions were estimated using least-squares minimization. This expansion technique greatly reduces the number of parameters needed to be estimated and thus estimation accuracy could be achieved even when applied to relatively short data recordings with the presence of noise. The least-squares minimization was repeated for different combinations of delays, number of MBF, and order of generalization. For each combination, the minimum description length (MDL) [8] was computed. MDL measures the relative quality of data fitting by balancing the goodness of fit and the complexity of the model. The set of parameters with the global minimum MDL is selected as the optimal set. Once all the parameters were determined, the kernels could be obtained using (3)-(5).

B. Simulated Data

To test the performance of the minimal models, we investigated three aspects of the estimation. The first aspect was to evaluate the accuracy of the estimated kernels of the linear model. The estimation algorithm was applied on the "data" generated by the simulation model. Details on the generation of simulated data are discussed in [6]. The estimated kernels were then compared with the "true" (simulated) kernels in the simulation model. To test how the level of noise affected the accuracy of the estimation, the estimation algorithm was applied on simulated data with different levels of system noise and measurement noise.

The second aspect was to investigate how nonlinearity in the simulation model affected the estimated kernels of the 2nd-order nonlinear model. To induce more nonlinearity to the simulated data, the linear operating range of the TPR baroreflex in the simulation model was lowered. The estimation algorithm of the nonlinear model was then applied on the simulated data from the original simulation model as well as the simulated data with the modified baroreflex control of TPR. The estimated kernels, the nonlinear kernels in particular, obtained from the original simulation model were then compared with the estimated kernels from the simulation model with the modified TPR baroreflex control.

Lastly, we determined the relationship between the gains in the simulation model and the system gains derived from the estimated linear kernels. The system gains were obtained by taking the Fourier transform of the kernels. The average of the magnitude part of the Fourier transform were taken in the low-frequency (0.04-0.15 Hz) and high-frequency (0.15-0.4 Hz) ranges. These derived system gains were then compared with the respective gains in the simulation model.

C. Experimental Data

Data from ten obese male pediatric subjects who underwent autonomic function tests, metabolic tests and sleep studies were used in this study. The experimental procedures included 1) noninvasive measurements of respiratory airflow, ECG, continuous blood pressure and PAT during supine and standing postures (10-min recording per posture); 2) morning fasting blood samples, followed by a frequently sampled intravenous glucose tolerance test; and 3) polysomnography. To investigate the effect of MetS + OSAS on autonomic reactivity due to orthostatic stress, the subjects were divided into 2 groups by their obstructive apnea hypopnea index (OAHI) and insulin sensitivity (SI). The subjects with lower OAHI and higher SI were treated as controls while the rest were treated MetS + OSAS subjects. The minimal models were applied on the experimental data

and the system gains were derived from the estimated kernels. The reactivity was defined as the percentage change in BPC and RPC gains in both low- and high-frequency ranges from supine to standing. *t*-test (or Mann-Whitney rank sum test) was employed to test the difference in reactivity between the two subject groups.

III. Results

A. Simulated Data – Effect of Noise

The estimation of the impulse responses was robust to the effect of measurement noise. With low level of system noise in the simulation model, the estimation was not accurate. The linear minimal model was able to recover the h_{RPC} well. The estimated h_{BPC} showed the initial negative response but the second peak of the estimated h_{BPC} closely resembled "true" h_{BPC} in terms of shape as well as time delay (Fig 1).

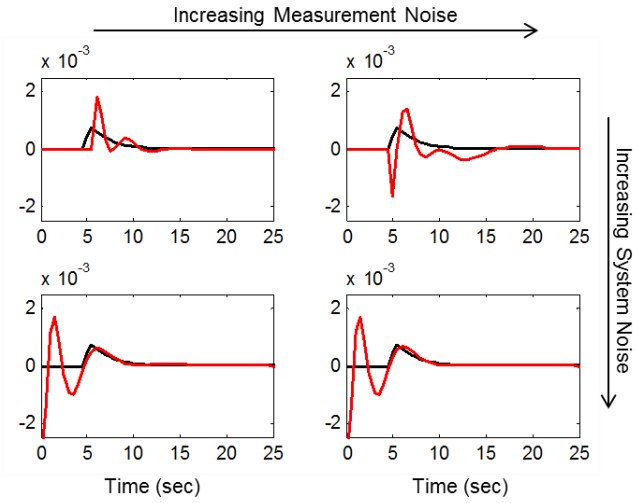

Figure 1. "True" (black) and estimated h_{BPC} (red) from simulated data with different levels of measurement and system noise.

B. Simulated Data – Increased Nonlinearity

Fig. 2 shows the estimated h_{2BPC} kernels from simulated data from the original simulation model and the simulation model with increased nonlinearity in the TPR baroreflex. The dynamics of the h_{2BPC} estimated from the simulation with increased nonlinearity was much larger compared to the h_{2BPC} estimated from the original simulation model.

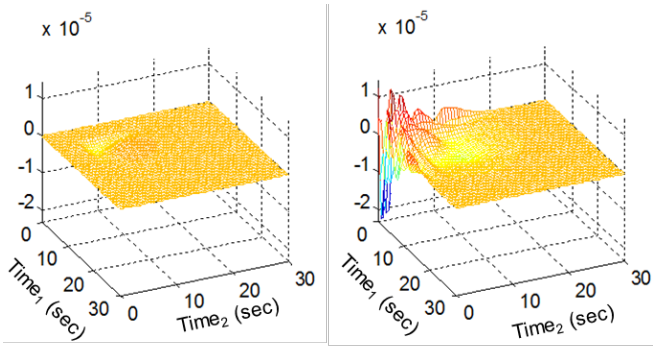

Figure 2. Estimated h_{2BPC} from the original simulation model (left) and the simulation model with increased nonlinearity in the TPR baroreflex (right)

C. Simulated Data – Simulated Gains vs. System Gains

Fig. 3 shows how the system gains derived from the estimated kernels changed with different levels of the simulated gains. Both low- and high-frequency BPC gains were linearly correlated with the simulated TPR baroreflex gain ($K_{b,TPR}$). As the $K_{b,TPR}$ increased, BPC gains in both frequency ranges also increased. The low-frequency BPC gain was more sensitive to the change the $K_{b,TPR}$ as reflected by steeper slope compared to the high-frequency BPC gain. Similar to the BPC gains, the RPC gains in both frequency ranges increased with increasing simulated gain of the sigh-vasoconstriction reflex (K_{RPC}). The low-frequency RPC gain showed linear correlation with K_{RPC}. However, the high-frequency RPC gains showed saturation effect as the simulated gain became lower.

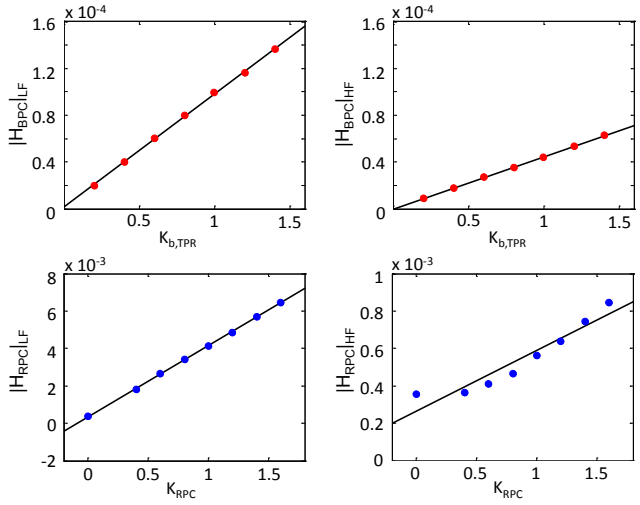

Figure 3. Simulated gains vs. system gains derived from the estimated linear kernels at low- and high-frequency ranges.

D. Experimental Data

TABLE I. Subject Characteristics

	***Control* (N = 5)**	***MetS + OSAS* (N = 5)**	***P-Value***
Age (years)	13.0 ± 3.0	13.9 ± 2.5	0.625
BMI (kg/m^2)	33.06 ± 4.64	38.28 ± 10.0	0.322
OAHI (events/hr)	1.94 ± 0.24	5.86 ± 2.66	0.008†
SI ($\times 10^{-4}$ min^{-1}/μU/ml)	6.60 ± 8.80	1.70 ± 0.68	0.222†

† Mann-Whitney rank sum test; otherwise, *t*-test
Data show mean ± standard deviation.

The subject characteristics are displayed in Table I. Overall, the system gains derived from both linear and nonlinear models decreased from supine to standing. For the gains derived from the linear model, the changes in the gains (measuring autonomic reactivity) of the control and MetS + OSAS groups were not significantly different. However, there was a significant difference in the change in high-frequency linear BPC gains derived from the nonlinear model. MetS + OSAS subjects show significantly larger reduction in the gains from supine to standing compared to the control subjects ($p = 0.016$). Similarly, there was a

greater reduction in the low-frequency 2nd-order nonlinear BPC gains from supine to stand in MetS + OSAS subjects compared to the control subjects. ($p = 0.039$). Fig. 4 shows the BPC gains derived from the nonlinear model from supine to standing in both subject groups.

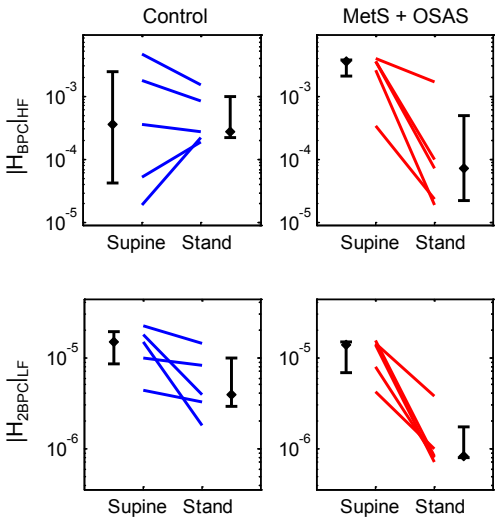

Figure 4. Nonlinear-model BPC gains from supine to standing across subject groups. (Error bars show median and interquartile range.) MetS + OSAS showed significant BPC gain reduction compared to controls.

IV. Discussion

To validate the accuracy of the kernel estimation, we applied the minimal model estimation to the simulated "data" produced by the simulation model developed in the previous study [6]. The estimated kernels were then compared with the kernels derived from the associated components of the simulation model. We found that higher system noise improved the estimation and the estimation was robust to the effect of measurement noise. The minimal model was able to recover the h_{RPC} accurately. The estimated h_{BPC} show the initial negative response. However, there was a positive peak at 5 seconds with the shape and dynamics that are comparable to the simulated impulse response. The negative peak in the estimated h_{BPC} could be attributed to the strong feedforward effect (vasoconstriction → increase in MAP).

Next, to validate whether the 2nd-order nonlinear minimal model was able to capture the nonlinear behavior in the system, the nonlinearity in the TPR baroreflex was increased by narrowing the linear operating range. We demonstrated the increased in nonlinearity could be reflected in the 2nd-order nonlinear BPC component, which showed much larger amplitudes compared to the nonlinear kernel estimated from the original simulation model.

To test whether there was a relationship between the system gains derived from the estimated kernels and the actual gains in the system, we adjusted the TPR baroreflex gains and RPC gains in the simulation model then compare these simulation gains with the system gains derived from the estimated kernels. We demonstrated that the system gains derived from the estimated kernels reflected the corresponding changes in the simulation gain. Further, even if the estimation of the h_{BPC} was not perfectly accurate, the derived BPC gains still showed good relationship with the simulation gains. This finding suggests that we could use the derived system gains as the compact descriptors of the autonomic function.

The linear and nonlinear minimal models were applied on experimental data collected from obese male pediatric subjects with mild (control) versus more severe degrees of MetS + OSAS. The system gains derived from the linear model could not differentiate the autonomic reactivity between the two subject groups. On the other hand, the system gains derived from the nonlinear model were able to differentiate the autonomic reactivity due to orthostatic stress between the control and MetS + OSAS subjects.

V. Conclusion

The linear minimal model of G_{PV} variability was able to recover the "true" impulse responses reasonably well. The nonlinear minimal model of G_{PV} was able to detect the increased nonlinearity in the system. The system gains derived from the estimated kernels could potentially serve as the compact descriptors of the autonomic function. The preliminary results show that the nonlinear minimal model was able to detect the difference in autonomic reactivity between control and MetS + OSAS subjects.

Acknowledgment

We thank F.M. Oliveira, W.H. Tran, and S.L. Davidson Ward for providing the experimental data used in this paper.

References

[1] S. C. Malpas, B. L. Leonard, S. J. Guild, J. V. Ringwood, M. Navakatikyan, P. C. Austin, G. A. Head, and D. E. Burgess, "The sympathetic nervous system's role in regulating blood pressure variability," IEEE Eng Med Biol Mag, vol. 20, no. 2, pp. 17-24, Mar-Apr, 2001.

[2] D. L. Eckberg, "Respiratory Sinus Arrhythmia and Other Human Cardiovascular Neural Periodicities," Regulation of Breathing, Lung Biology in Health and Disease J. A. Dempsey and A. I. Pack, eds., pp. 669-740, New York: Marcel Dekker, 1995.

[3] D. R. Seals, N. O. Suwarno, M. J. Joyner, C. Iber, J. G. Copeland, and J. A. Dempsey, "Respiratory modulation of muscle sympathetic nerve activity in intact and lung denervated humans," Circulation research, vol. 72, no. 2, pp. 440-54, Feb, 1993.

[4] B. Bolton, E. A. Carmichael, and G. Sturup, "Vaso-constriction following deep inspiration," J Physiol, vol. 86, no. 1, pp. 83-94, Jan 15, 1936.

[5] S. Sangkatumvong, M. C. Khoo, R. Kato, J. A. Detterich, A. Bush, T. G. Keens, H. J. Meiselman, J. C. Wood, and T. D. Coates, "Peripheral vasoconstriction and abnormal parasympathetic response to sighs and transient hypoxia in sickle cell disease," Am J Respir Crit Care Med, vol. 184, no. 4, pp. 474-81, Aug 15, 2011.

[6] P. Chalacheva, and M. C. Khoo, "An extended model of blood pressure variability: Incorporating the respiratory modulation of vascular resistance," Conf Proc IEEE Eng Med Biol Soc, vol. 2013, pp. 3825-8, 2013.

[7] J. A. Jo, A. Blasi, E. M. Valladares, R. Juarez, A. Baydur, and M. C. Khoo, "A nonlinear model of cardiac autonomic control in obstructive sleep apnea syndrome," Ann Biomed Eng, vol. 35, no. 8, pp. 1425-43, Aug, 2007.

[8] J. Rissanen, "Estimation of structure by minimum description length," Circ Syst Sig Process, vol. 1, pp. 395-406, 1982.